ChemPubSoc Europe

DOI: 10.1002/chem.201304851

CHEMISTRY
A European Journal
Full Paper

Supramolecular Chemistry

Recognition of Free Tryptophan in Water by Synthetic Pseudopeptides: Fluorescence and Thermodynamic Studies

Vicente Martí-Centelles, M. Angeles Izquierdo, M. Isabel Burguete, Francisco Galindo,* and Santiago V. Luis*[a]

Abstract: Pseudopeptidic receptors containing an acridine unit have been prepared and their fluorescence response to a series of amino acids was measured in water. Free amino acids, not protected either at the C or the N terminus, were used for this purpose. The prepared receptors display a selective response to tryptophan (Trp) versus the other assayed amino acids under acidic conditions. The macrocyclic nature of the receptor is important as the fluorescence quenching is higher for the macrocyclic compound than for the related open-chain receptor. Notably, under the experimental acidic conditions used, both the receptor and guest are fully protonated and positively charged; thus, the experimental results suggest the formation of supramolecular species that contain two positively charged organic molecular components in proximity stabilized through aromatic–aromatic interactions and a complex set of cation-anion-cation interactions. The selectivity towards Trp seems to be based on the existence of a strong association between the indole ring of the monocharged amino acid and the acridinium fragment of the triprotonated form of the receptor, which is established to be assisted by the interaction of the cationic moieties with hydrogen sulfate anions.

Introduction

Amino acids are essential building blocks for living organisms as they are the structural basis of proteins and peptides. In this regard, supramolecular interactions that involve amino acids, peptides, and proteins are of paramount importance as, for instance, the protein–protein interaction is an important process in cell recognition.[1–3] On the other hand, the aggregation of peptides and proteins is a well-known phenomenon, which is sometimes linked to disease states.[4] Hence, the understanding of such weak association process within the framework of supramolecular chemistry, under natural and non-natural conditions, is of fundamental importance.[2,5–10] In this context, the recognition of amino acids and amino acid-related compounds has attracted the attention of numerous researchers from a basic perspective, but also from an applied point of view.[11–14] A growing number of reports that deal with the bioanalysis of amino acid mixtures have been published in recent years.[15–30] Some diagnostic assays are based on photoinduced electron-transfer processes that involve one or more target amino acids.[31–33] However, despite the great development experienced by the bioanalytical sciences in the use of fluorescence-based techniques, a current challenge is still the lack of knowledge about many elementary interactions that occur at the level of a single amino acid under the considered experimental conditions. An illustrative example was provided recently by Webb and co-workers, who described how free tryptophan can dramatically quench the emission of the popular probe Alexa 488.[34] Interestingly, half of the quenching was shown to arise from a ground-state association of the probe and the amino acid.

The development of methods for the recognition and sensing of amino acids is vital because of their critical biological relevance,[18,23,34–37] which is particularly true for the sensing of tryptophan.[20,30,38–41] The presence of tryptophan is directly related to the immune system, in which enzymes break down this amino acid through the kynurenine metabolic pathway.[42,43] Tryptophan is required for protein synthesis and other important metabolic functions; in addition, this amino acid is the only source for the production of several important molecules in the nervous system, such as serotonin, whereas tryptophan is used for the synthesis of melatonin in the pineal gland.[42,44]

Taking into account the importance of basic studies that have tackled the interaction between amino acids and small fluorescent molecules and our previous work on pseudopeptidic supramolecular systems,[45] we report herein supramolecular studies on a series of acridine-based pseudopeptidic molecules (Figure 1) with different unprotected amino acids by means of NMR, UV/Vis, and fluorescence (steady-state and time-resolved) spectroscopy and computational calculations. The complexation of such receptors with free amino acids has

[a] Dr. V. Martí-Centelles, Dr. M. A. Izquierdo, Dr. M. I. Burguete, Dr. F. Galindo, Dr. S. V. Luis
Departamento de Química Inorgánica y Orgánica
Universitat Jaume I, Av. Sos Baynat, s/n
E-12071 Castellón (Spain)
Fax: (+34) 964728214
E-mail: francisco.galindo@uji.es
luiss@uji.es

Supporting information for this article is available on the WWW under http://dx.doi.org/10.1002/chem.201304851.

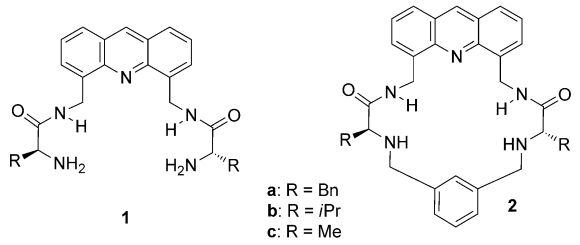

Figure 1. The pseudopeptidic receptors containing acridine fragments considered herein.

been studied. These pseudopeptidic receptors selectively recognize free tryptophan (Trp) over alanine (Ala), histidine (His), methionine (Met), phenylalanine (Phe), tyrosine (Tyr), and valine (Val). Even at a very low pH values, receptors **1** and **2** and Trp can associate to an appreciable extent, most likely with the participation of aromatic interactions, which is remarkable considering that both the receptor and the host are positively charged.[46]

Results and Discussion

Recognition studies were carried out with four pseudopeptidic synthetic receptors based on Val and Phe **1a**,**b** and **2a**,**b**, respectively, and seven free amino acids (i.e., Ala, His, Met, Phe, Tyr, Trp, and Val) as guests.

Synthesis of the receptors

The design of the acridine pseudopeptides considered herein is based on our previous studies that revealed how this type of molecule represents an interesting option for anion recognition and fluorescent sensing, in particular in acidic media.[47] The presence of aromatic **1a** and **2a** and nonaromatic **1b** and **2b** side chains was considered to be an interesting design vector because these side chains can participate in different types of interaction. The synthesis of receptors **1a** and **2a** and their actuation as selective fluorescent sensors for $H_2PO_4^-$ ions has been described previously.[47] An analogous procedure was followed for the synthesis of **1b** and **2b** (Scheme 1). The synthesis of the pseudopeptidic compound **1b-Cbz** was carried out by reaction of 4,5-bis(aminomethyl)acridine with the corresponding protected amino acid activated as its hydroxysuccinimide ester with dimethoxyethane (DME) as the solvent. 4,5-Bis-(aminomethyl)acridine was prepared according to previously reported procedures.[48–51] The carbobenzlyoxy (Cbz) protecting group was removed by using an HBr/AcOH mixture followed by neutralization with NaOH to yield the open-chain receptor **1b**. The most difficult step in the synthetic scheme is the macrocyclization reaction to obtain macrocycle **2b**. In this case, careful control of the temperature, with the use of a temperature gradient[47,52] and under conditions similar to those used for related pseudopeptidic macrocycles, provided significantly better yields than by performing the reaction at reflux. Thus, macrocycle **2b** was prepared from the reaction of bis(amino amide) **1b** with 1,3-bis(bromomethyl)benzene in acetonitrile in

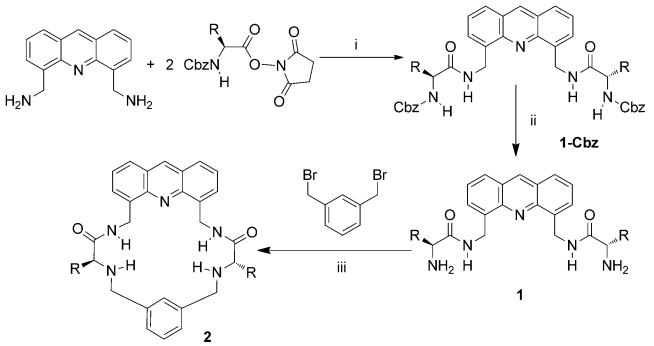

Scheme 1. Synthesis of pseudopeptidic receptors **1** and **2**. i) DME; ii) HBr/AcOH 33%, RT then aq. NaOH; iii) TBABr, DIPEA, CH_3CN, temperature gradient = 50–81 °C.

the presence of tetrabutylammonium bromide (TBABr) and *N,N*-diisopropylethylamine (DIPEA) with a temperature gradient of 50–81 °C. The crude product was purified by column chromatography to afford the pure macrocycle in 63% yield, which is a remarkable yield taking into account that high dilution conditions were not employed.[53,54] These relatively high yields obtained for the macrocyclization reaction suggest a high degree of preorganization of the open-chain intermediate and the corresponding transition state, which has been demonstrated in other cases that used this methodology.[55–60]

Characterization of compounds

Compounds **1b** and **2b** were characterized by spectroscopic and analytical techniques. Interestingly, in solution with $CDCl_3$, the ^{1}H NMR signals of the CH_2 groups at positions 4 and 5 of the acridine moiety are remarkably different for the open-chain derivatives **1a**,**b** and macrocyclic derivatives **2a**,**b**. For the open-chain compound **1a**, these protons appear as one doublet, whereas in **1b**, **2a**, and **2b** they appear as two double doublets. This finding points to the presence of an appreciable coupling constant with the amide hydrogen atom in **1b**, **2a**, and **2b** (see Figure 2 and Figure S20 in the Supporting Information). This effect is higher for the macrocyclic compounds, which is expected for compounds with higher conformational restrictions. However, it is remarkable that an analogous pattern can also be observed for the open-chain compound **2a**. Thus, the conformational freedom of this Val-derived compound is notably restricted relative to the Phe-derived analogue **1a** (compare spectra (a) and (c) in Figure 2). This behavior can be associated to the higher rigidity provided by the Val side chain (isopropyl) relative to the Phe side chain (benzyl) according to the conformational-flexibility scale for amino acids proposed by Huang and Nau,[61] in which Val is only surpassed in rigidity by isoleucine (Ile) and especially by proline (Pro).

The electronic absorption spectra and the steady-state fluorescence emission spectra of **1b** and **2b** were also recorded in $CHCl_3$. As expected,[62] **1b** and **2b** have similar properties, thus showing absorption maxima at $\lambda = 357$ nm and an emission

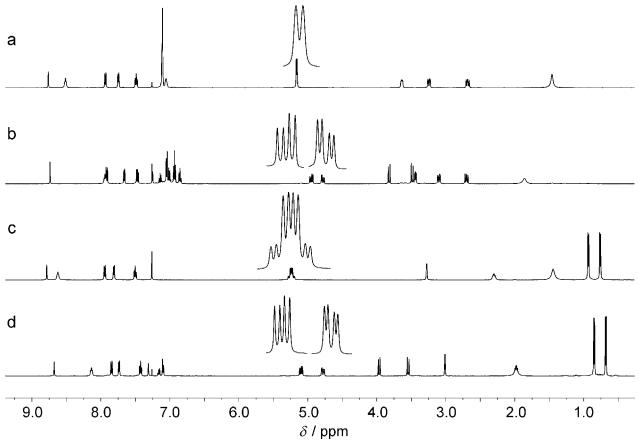

Figure 2. ^{1}H NMR spectra (20 mM, $CDCl_3$) of compounds: a) **1a**, b) **1b**, c) **2a**, and d) **2b**.

maximum at $\lambda = 420$ nm when excited at $\lambda = 357$ nm (Figure 3; see ref. [47] for the related compounds **1a** and **2a**).

The fluorescence quantum yields for **1b** and **2b** at acidic pH values were similar (pH 0.37 and 0.36, respectively) to those reported for **1a** and **2a** (pH 0.43 and 0.38, respectively),[47] and all of them slightly lower than those measured for the parent acridine (pH 0.65).[62] The quantum yield significantly decreases upon increase of the pH value, which is expected from the conversion of a highly emissive fluorophore such as acridinium (Figure 4) into the less emissive acridine.[63–67] In addition, time-correlated single-photon counting (TCSPC) was used to characterize the singlet excited states of **1b** and **2b**. Values for the different fluorescence lifetimes τ_F were obtained by the fitting the data to the equation $I = I_0 \Sigma \alpha_i \tau_i$ (see Figure S10 in the Supporting Information). From the excitation and emission curves, the energy of the singlet excited state E_S was also calculated for each compound (Table 1).

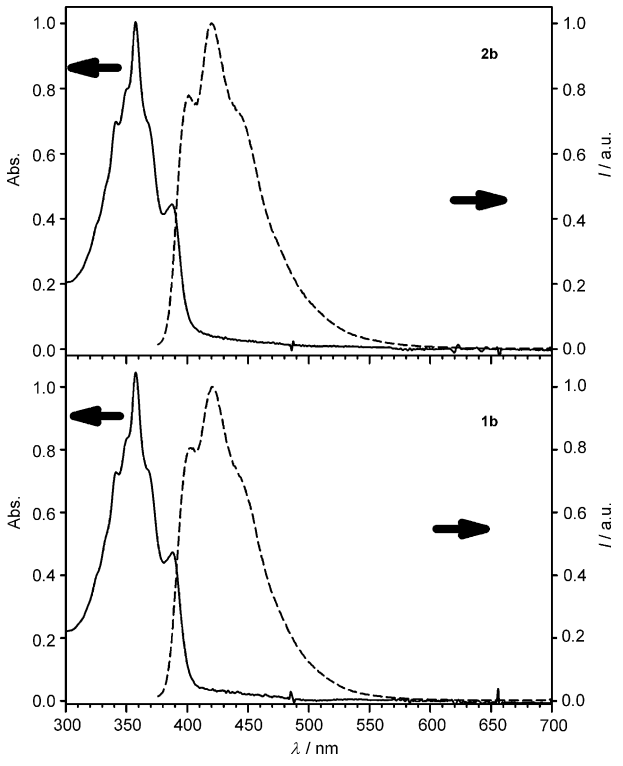

Figure 3. Normalized absorption (left axis) and emission (right axis) spectra for **1b** and **2b** in $CHCl_3$. $\lambda_{ex} = 357$ nm. Probe concentration = 10 μM.

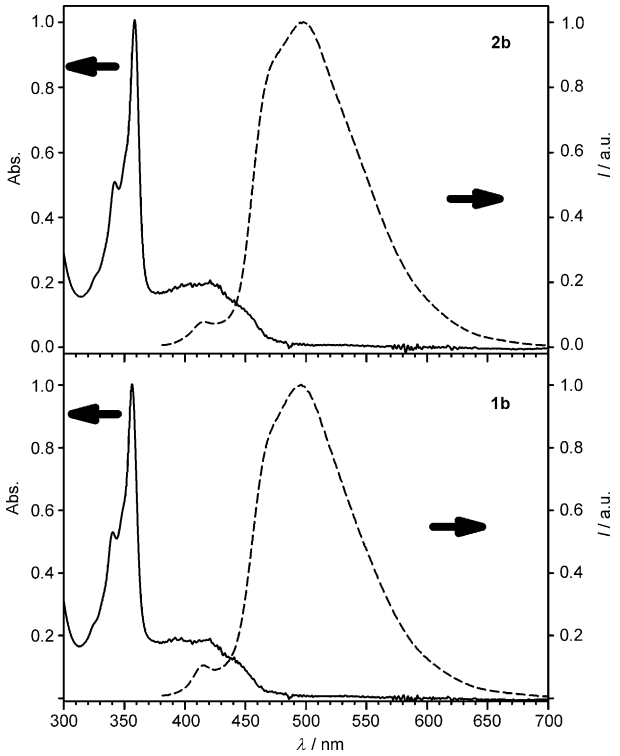

Figure 4. Normalized absorption (left axis) and emission (right axis) spectra for **1b** and **2b** in H_2O at pH 1.00. $\lambda_{exc} = 357$ nm. Probe concentration = 20 μM.

The behavior of pseudopeptidic compounds **1** and **2** in an acidic medium is comparable to that displayed by acridine, that is, the emitting species at long wavelengths is clearly the protonated acridine species (acridinium cation), which displays fluorescence properties (E_S = ca. 62–66 kcal mol^{-1} and τ_1 = ca. 24–32 ns) clearly different to the acridine moiety (E_S = ca. 72 kcal mol^{-1} and $\tau_1 = < 10$ ns).[47,62,64]

Determination of pK_a values

The pK_a values for the protonation at the acridine moiety of these compounds were determined by means of fluorescence titrations. The variation in the intensity of the fluorescence emission of the acridinium moiety (excitation wavelength at isosbestic points: $\lambda = 363$ and 365 nm for **1b** and **2b**, respectively) at different pH regions was used to determine the pK_a values for the protonation of the acridine moiety in the receptors by fitting the corresponding fluorescence intensity versus the pH value for each titration (Figure 5).

The on/off fluorescence switching process at very low pH values corresponds to the protonation of the nitrogen atom of the acridine ring because the aliphatic amines should

Table 1. Fluorescence properties for **1** and **2** in water (measurements made with a concentration of 20 μM in water using H_2SO_4 and NaOH to adjust the pH.)

	pH	λ_{abs} [nm]	λ_{exc} [nm]	λ_{em} [nm][a]	ES_1 [kcal mol^{-1}]	Φ_F[b]	τ_1 [ns][c]	α_1 [%]	τ_2 [ns][c]	α_2 [%]	χ^2	pK_a
Acridine	0.92	354, 398	354[d]	477	65.9	0.65	31.6[e]	–	–	–	1.03	5.42[f]
	12.65	355	354[g]	427	72.7	0.24	9.5[h]	–	–	–	1.22	
2a[i,j]	0.55	359, 397	359[d]	502	62.7	0.38	23.9[e]	–	–	–	1.15	1.67 ± 0.02
1a[j]	0.68	358, 398	359[d]	501	62.6	0.43	26.6[e]	–	–	–	1.15	2.74 ± 0.01
	4.16	357	356[k]	432	71.8	0.05	1.3[h]	95.4	12.2[h]	4.6	0.96	
2b	0.24	358, 420	357[d]	504	62.2	0.36	20.8[e]	–	–	–	0.92	2.47 ± 0.01
	4.05	356	356[l]	437	71.4	0.03	1.1[h]	78.4	12.4[h]	21.6	0.83	
1b	0.30	356, 416	355[d]	501	62.8	0.37	22.4[e]	–	–	–	1.02	2.63 ± 0.02
	4.13	356	355[l]	428	70.4	0.03	1.1[h]	58.4	12.5[h]	41.6	0.88	

[a] λ_{exc} = 366 nm. [b] Quinine sulphate standard (aqueous H_2SO_4 0.1 M, air); Φ_F = 0.53 (taken from ref. [67]). [c] λ_{exc} = 372 nm. [d] λ_{em} = 540 nm. [e] λ_{em} = 475 nm. [f] Taken from ref. [63]. [g] λ_{em} = 470 nm. [h] λ_{em} = 426 nm. [i] It was not possible to measure this sample at pH 4 due to precipitation of the product. [j] Taken from ref. [47]. [k] λ_{em} = 450 nm. [l] λ_{em} = 490 nm.

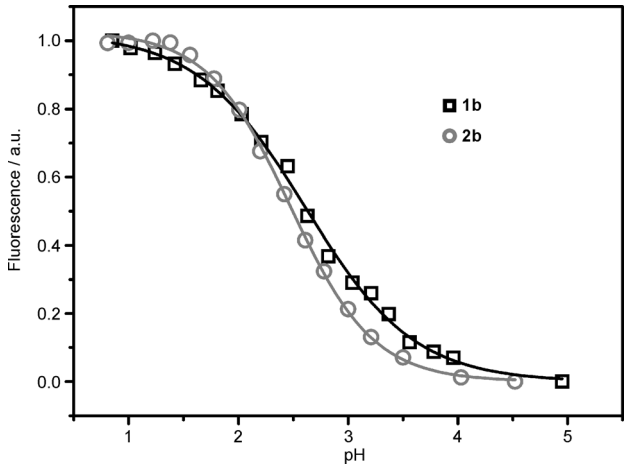

Figure 5. Fluorescence pH titrations of **1b** and **2b** that monitor the emission at λ = 495 and at 500 nm for **1b** and **2b**, respectively. Probe concentration = 10 μM in aqueous solution (1% DMSO). λ_{ex} = 363 and 365 nm and pK_a = 2.63 ± 0.02 and 2.47 ± 0.01 for **1b** and **2b**, respectively.

protonate first due to their primary and secondary character (i.e., **1b** and **2b**, respectively). This behavior is comparable with examples reported, for instance, for polyaza pyridinophanes able to admit up to six protons, including the protonation of the nitrogen atom at the pyridine moiety.[68]

By comparing these pK_a values for compounds derived from Val **1b** and **2b** and from Phe **1a** and **2a**, some differences can be observed, especially for macrocycles **2a** and **2b** (pK_a = 1.67 vs 2.47). Most likely, this difference reflects the different hydrophobicity imparted by the side chains, as previously studied for analogous compounds.[59,60]

Recognition of amino acids

^{1}H NMR experiments

To analyze the ability of these pseudopeptidic compounds to interact with amino acids, different ^{1}H NMR spectroscopic experiments were carried out. It is worth mentioning that previous work by our group has focused on the study of *N*-protected amino acids and dipeptide recognition by related pseudopeptidic receptors.[23,59,69] In this case, however, the study was based on the recognition of amino acids not derivatized as esters or protected with carbamate groups, which is more relevant from a biomedical point of view, in particular for the development of sensing methodologies of practical interest. The free amino acids considered here (i.e., Ala, His, Met, Phe, Trp, Tyr, and Val; Figure 6) are expected to exist as zwitterions at neutrality[15] or as cationic species at the experimental acidic pH values required for the protonation of the acridine fragment.

The most interesting results were observed at acidic pH values. Titrations of **1a** and **2a** with the different amino acids were performed in D_2O (2 M H_2SO_4) with *tert*-butanol as an internal standard (Figures 7 and 8). Studies

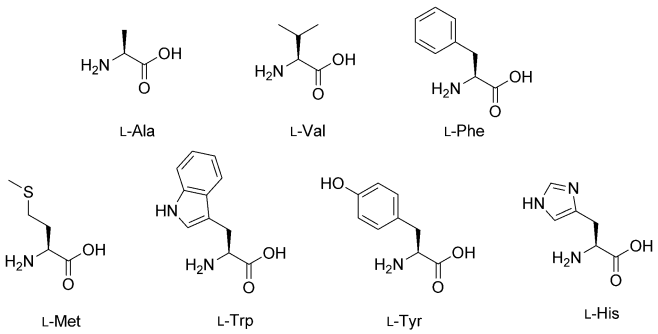

Figure 6. The L-amino acids considered herein.

carried out with L-Trp were the most significant. For both receptors, the ^{1}H NMR signal of the acridine H9 atom displayed a large upfield shift upon the addition of L-Trp ($\Delta\delta_{max}$ = −0.999 ppm). This shift suggests the presence of an important interaction between L-Trp and **1a** and **2a**, which could take place by π–π stacking between the electron-poor acridinium cationic fragment and the electron-rich indole ring. In sharp contrast, ^{1}H NMR titration experiments with L-Met showed a very small downfield shift ($\Delta\delta$ = 0.015 ppm for the last point of the titration ([L-Met] = 0.125 M)) for the same signal. Experiments with L-Tyr also showed a small upfield change. Finally, experiments with Ala, Phe, His, and Val did not show any varia-

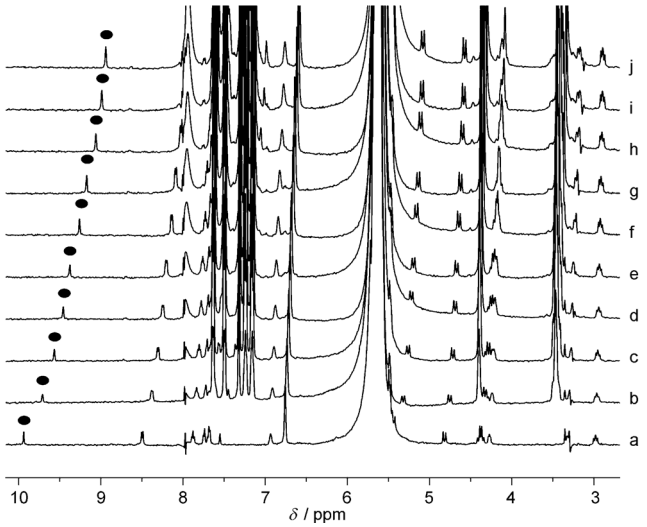

Figure 7. ^{1}H NMR titration of **2a** (5 mM) with L-Trp (from 0 to 0.25 M) in 2 M H_2SO_4 in D_2O. The acridine H9 signal, which is upfield shifted with the addition of Trp, is marked with a black dot: a) 0, b) 24, c) 45, d) 65, e) 83, f) 115, g) 143, h) 188, i) 222, j) 250 mM Trp.

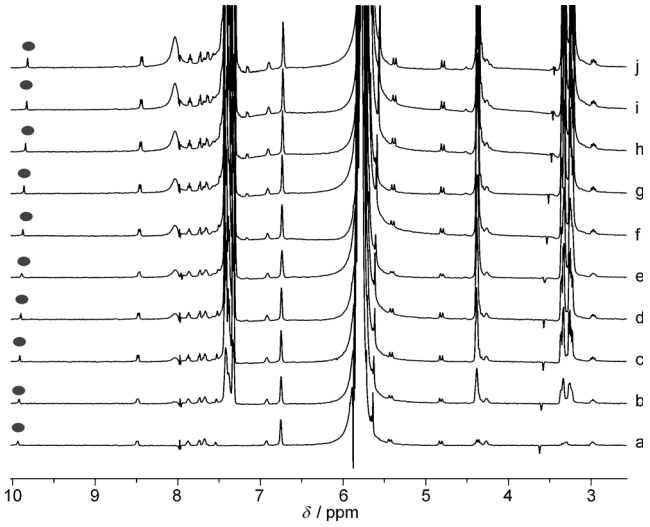

Figure 8. ^{1}H NMR titration of **2a** (5 mM) with L-Phe (from 0 to 0.25 M) in 2 M H_2SO_4 in D_2O. The acridine H9 signal, which is upfield shifted with the addition of Trp, is marked with a black dot a) 0, b) 24, c) 45, d) 65, e) 83, f) 115, g) 143, h) 188, i) 222, j) 250 mM Phe.

tion in the ^{1}H NMR chemical shifts, thus indicating that no noticeable association between the host and guest takes place, which can be observed in Figure 8 for the titration of macrocycle **2a** with L-Phe.

Fluorescence quenching studies

To gain further insight into the association process detected for Trp, fluorescence and UV/Vis titration experiments were performed under related experimental conditions (1 M H_2SO_4). Both the UV/Vis and fluorescence spectra displayed appreciable changes with the addition of Trp that which were more significant than those observed with other amino acids. Strong quenching of the fluorescence emission of **1** and **2** was only detected in the case of Trp (Figure 9), only slightly quenched by Tyr and Met, and not quenched at all by Ala, Val, Phe, or His.

Stern–Volmer analysis [Eqs (1) and (2)] of the fluorescence quenching allows its nature to be determined, hence disclosing dynamic (collisional) and static (ground-state association) effects.[70,71] Theoretically, pure dynamic quenching provides a linear Stern–Volmer plot from the quenching experiments from steady-state emission measurements [Eq. (1)], whereas a deviation from linearity indicates an interaction between the host and the guest in the ground state and Equation (2) applies.[72] The dynamic quenching constant is related to the excited-state lifetime according to Equation (3). Plot deviation from the linearity in the plot obtained:

$$\tau_0/\tau = I_0/I = 1 + K_D[Q] \quad (1)$$

$$I_0/I = (1 + K_D[Q])(1 + K_S[Q]) \quad (2)$$

$$K_D = k_q\tau \quad (3)$$

where τ_0 is the fluorescence lifetime in the absence of a quencher, τ is the fluorescence lifetime in the presence of a quencher, I_0 is the fluorescence emission intensity in the absence of a quencher, I is the fluorescence emission intensity in the presence of a quencher, K_D is the dynamic quenching constant, K_S is the static quenching constant, and k_q is the dynamic rate quenching constant.

The fluorescence emission intensity of the receptor was measured in the presence of increasing concentrations of the different amino acids in acidified water (1 M H_2SO_4; see Figure S18 in the Supporting Information). Under such acidic conditions, the receptors are triprotonated[47] and the amino acids are monoprotonated.[73,74] Amino acids that contain an aliphatic side chain (L-Ala, L-Val), a benzene ring (L-Phe), or a protonated imidazole ring (L-His) did not disturb the fluorescence emission of the receptors. On the contrary, those containing electron-rich side chains (L-Trp, L-Tyr, L-Met) quenched the fluorescence intensity of the receptors, although with remarkable differences, with Trp displaying the most marked effect. The quenching was nonlinear as the Stern–Volmer plot curved upwards. This deviation from linearity indicates a combination of both dynamic and static quenching processes, that is, the existence of an effective complexation in the ground state as suggested by NMR spectroscopic experiments. Titrations were carried out for both enantiomers of each amino acid (see Figure S18 in the Supporting Information), but no appreciable enantiodifferentiation was detected.

Additionally, time-resolved fluorescence experiments for the titration of the hosts **1a**, **2a**, **1b**, and **2b** with Trp were also performed to confirm the coexistence of static and dynamic quenching. In this type of experiment, only the dynamic quenching of the excited state is observed, thus allowing the calculation of the corresponding dynamic quenching constant K_D. Therefore, the combination of time-resolved and steady-state fluorescence experiments allowed determination of the

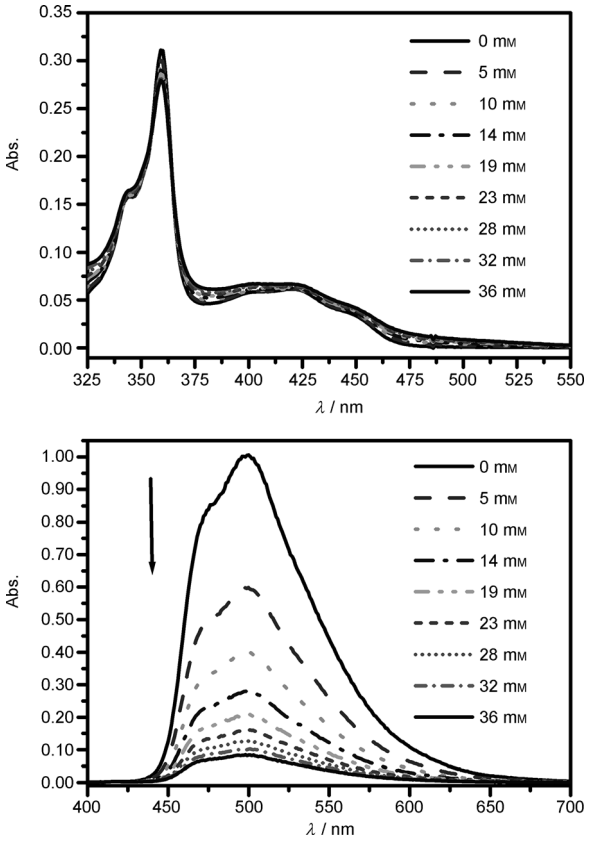

Figure 9. Variation of the fluorescence and absorbance in the titration of **2a** (20 μM) with L-Trp (from 0 to 36 mM) in H_2SO_4 (1 M).

K_D and K_S quenching constants. As an example, Figure 10 shows the fluorescence-decay curves for the titration of **2a** with L-Trp.

Both types of measurements can be combined in the same graph as for **2a** with L-Trp (Figure 11). It can be observed that the Stern–Volmer plot for the time-resolved fluorescence measurements fits to a straight line. On the other hand, the representation of the steady-state measurements shows an upward curvature that can be fitted to Equation (2) [(by using the previously calculated K_D constant from the time-resolved fluorescence fitting to Eq. (1)], thus allowing the calculation of the K_S constant. The latter process must be associated to the formation of a nonfluorescent complex in the ground state. By using the calculated K_S value, it is possible to obtain the associated Gibbs free energy ΔG,[75] which is approximately −1.0 kcal mol^{-1} in the case of L-Trp. The recognition process is slightly more favorable for the L enantiomer, although the enantiodiscrimination is low.

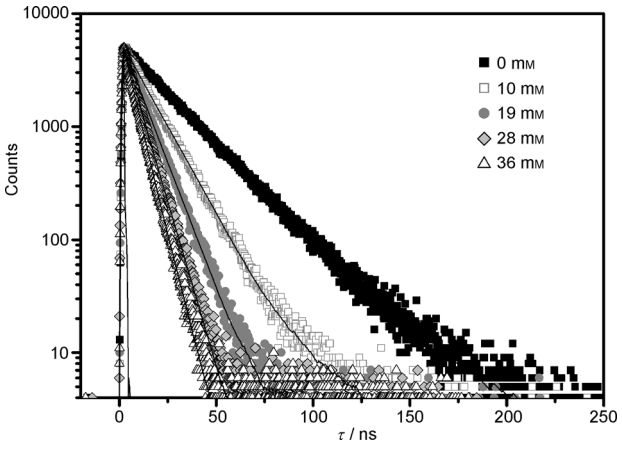

Figure 10. Fluorescence-decay curves for the titration of **2a** (20 μM) with L-Trp (from 0 to 36 mM) in aqueous H_2SO_4 (1 M). $\lambda_{ex}=372$, $\lambda_{em}=475$ nm.

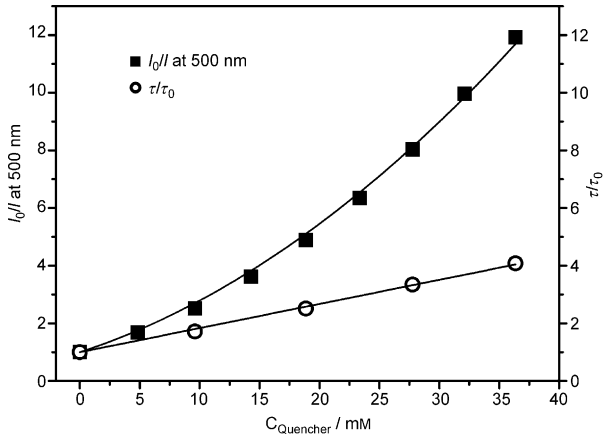

Figure 11. Stern–Volmer plot of the titration of **2a** (20 μM) with L-Trp (from 0 to 36 mM) in aqueous H_2SO_4 (1 M). Solid lines correspond to fitting to Equations (1) and (2). $\lambda_{ex}=366$ nm.

Following a similar methodology, fitting to the Stern–Volmer equations was performed for the different titrations (the results are summarized in Table 2). The most effective quencher was clearly Trp with a K_D constant of approximately 83–93 M^{-1} for **1a** and **2a**, whereas the K_D constant was approximately 60–75 M^{-1} for **1b** and **2b**. Therefore, the isopropyl side chain derived from Val in **1b** and **2b** seems to decrease the dynamic quenching constant relative to Phe-derived compounds. The same effect of the amino acid side chain in receptors **1** and **2** was also observed for Tyr and Met. Regarding the ground-state complexes, the K_S binding constants with Trp and Tyr are in the ranges 20–60 and 2–4 M^{-1}, respectively, and are negligible with Met. The observation of a moderate association constant with Trp in the ground state by means of fluorescence spectroscopy is in agreement with the chemical shifts recorded by using ^1H NMR spectroscopy, hence confirming the existence of a supramolecular complex with Trp. This finding is remarkable considering that quite extreme conditions were employed (i.e., 1 M H_2SO_4) and highlights the tendency of amino acids (in this case, Trp) to form supramolecular complexes, even in the most harsh environment. Remarkably, the association constants for the macrocyclic receptors are approximately 50% higher than for the open-chain compounds, which could be ascribed to the well-known macrocyclic effect (preorganization of hosts).[75]

From the calculated K_D constants, it is possible to obtain the corresponding dynamic quenching rate constants k_q by using Equation (3). Table 3 summarizes the obtained k_q constants for the fluorescence quenching of the studied acridine-based receptors, which are in the range $(2.0–3.9)\times10^9$ $M^{-1}s^{-1}$. For a typical small molecule in water, the diffusion rate is 7.4×

Table 2. Parameters obtained from fitting to Stern–Volmer plots from the titration of **1a**, **2a**, **1b**, and **2b** (20 μM) with a series of L- and D-amino acids (from 0 to 36 mM) in aqueous H_2SO_4 (1 M). $\lambda_{exc}=366$ nm.[a]

Aaa	[M^{-1}]	**1a**	**2a**	**1b**	**2b**
L-Trp	K_D [b]	86.5±1.7	83.7±1.2	74.0±0.2	59.1±1.2
	K_S [c]	32.5±0.3	52.0±0.8	32.1±0.4	59.2±0.5
D-Trp	K_D [b]	92.8±1.7	83.5±1.0	70.8±0.5	74.1±0.7
	K_S [c]	23.9±0.1	45.4±0.4	30.7±0.3	40.7±0.2
L-Met	K_D [d]	61.5±0.8	54.3±0.4	51.0±0.4	43.6±0.5
D-Met	K_D [d]	58.4±0.6	49.5±0.6	49.2±0.3	43.0±0.3
L-Tyr	K_D [e]	80.5±1.2	81.4±1.8	65.2±1.3	69.2±1.5
D-Tyr	K_D [e]	85.7±1.4	87.5±2.1	68.5±1.5	63.8±1.5
L-Tyr	K_D [f]	72.3±1.0	70.2±1.1	59.1±0.4	59.3±1.0
	K_S [g]	2.68±0.13	3.67±0.18	2.60±0.19	3.11±0.15
D-Tyr	K_D [f]	77.4±1.1	75.3±1.1	60.0±0.6	54.7±0.8
	K_S [g]	2.44±0.13	3.75±0.20	3.06±0.17	3.34±0.20

[a] Steady-state fluorescence experiments were measured at 500 nm for compounds **1a**, **2a**, and **2b**; and at 495 nm for compound **1b**. Studies with L-Ala, L-His, L-Val, and L-Phe indicated that these amino acids do not quench the fluorescence of **1a**, **1b**, **2a**, and **2b** under the used experimental conditions. [b] K_D obtained from fluorescence lifetime measurements. [c] K_S obtained from steady-state fluorescence measurements using the K_D constant. [d] K_D obtained from steady-state fluorescence measurements. [e] K_D obtained from steady-state fluorescence measurements to the first points; a small variation from the linearity of the fits was observed associated to a small binding constant. [f] K_D obtained from steady-state fluorescence measurements to the first points. [g] K_S obtained from steady-state fluorescence measurements using the K_D constant.

Table 3. Dynamic quenching constants k_q ($M^{-1}s^{-1}$) obtained from fittings to Stern–Volmer plots of the titration of **1a**, **2a**, **1b**, and **2b** (20 μM) with a series of L- and D-amino acids (from 0 to 36 mM) in aqueous H_2SO_4 (1 M).

Aaa	**1a** k_q [$M^{-1}s^{-1}$]	**2a** k_q [$M^{-1}s^{-1}$]	**1b** k_q [$M^{-1}s^{-1}$]	**2b** k_q [$M^{-1}s^{-1}$]
L-Trp	$(3.25\pm0.06)\times10^9$	$(3.50\pm0.05)\times10^9$	$(3.30\pm0.01)\times10^9$	$(2.84\pm0.06)\times10^9$
D-Trp	$(3.49\pm0.06)\times10^9$	$(3.49\pm0.04)\times10^9$	$(3.16\pm0.02)\times10^9$	$(3.56\pm0.03)\times10^9$
L-Met	$(2.31\pm0.03)\times10^9$	$(2.27\pm0.02)\times10^9$	$(2.28\pm0.02)\times10^9$	$(2.10\pm0.02)\times10^9$
D-Met	$(2.20\pm0.02)\times10^9$	$(2.07\pm0.03)\times10^9$	$(2.20\pm0.01)\times10^9$	$(2.07\pm0.01)\times10^9$
L-Tyr	$(2.72\pm0.04)\times10^9$	$(2.94\pm0.05)\times10^9$	$(2.64\pm0.02)\times10^9$	$(2.85\pm0.05)\times10^9$
D-Tyr	$(2.91\pm0.04)\times10^9$	$(3.15\pm0.05)\times10^9$	$(2.68\pm0.03)\times10^9$	$(2.63\pm0.04)\times10^9$
NaCl	$(2.74\pm0.02)\times10^8$	$(2.52\pm0.04)\times10^8$	$(7.19\pm0.01)\times10^8$	$(3.50\pm0.01)\times10^8$

$10^9\,M^{-1}s^{-1}$,[62] which is in agreement with the obtained results; therefore, these rates are about one half of the diffusion-controlled limit.[76] Sauer and co-workers reported bimolecular fluorescence quenching constants in the range $(2.0–5.0)\times10^9\,M^{-1}s^{-1}$ for several bioprobes that interact with Trp, which is in close agreement with our results. Additionally, a moderate association in the ground state has been described for those dyes with association constants in the range 96–206 M^{-1}.[38] More recently, Webb and co-workers described the fluorescence quenching of the bioprobe ALEXA 488 by Trp with a dynamic rate of $k_q=3.5\times10^9\,M^{-1}s^{-1}$; however, in that case, the association of the dye and the amino acid was weaker (15.1 M^{-1}) than in the present situation.[34]

Regarding the physical mechanism that results in the quenching of the fluorescence emission of the receptors by Trp, it is reasonable to consider the participation of the well-known process of photo-induced electron transfer (PET). The acridinium cation is an excellent oxidizing agent in the first excited state and, accordingly, the emission of acridinium and 9-methylacridinium cations has been described to be strongly quenched by electron-rich donors through PET with $k_q=(3.5–4.7)\times10^9\,M^{-1}s^{-1}$.[77] In our case, we calculated the feasibility of PET for Trp, Tyr, and Met to the pseudopeptidic receptors by using the Rehm–Weller formulation[78] (see the Supporting Information). In all the cases, the resulting ΔG values associated with the PET process are negative ($\Delta G=-20$, -15, and -7 kcal mol^{-1} for Trp, Tyr, and Met, respectively), which supports employing the PET mechanism to explain the emission quenching.

Thermodynamic studies

To understand the association process better, that is, whether it is entropy or enthalpy controlled, the association constants for **1a** and **2a** with L-Trp were determined by using UV/Vis titrations at different temperatures. The use of UV/Vis spectroscopy afforded values of K_S analogous to those obtained by fluorescence, but the absorption data were more robust for thermodynamic studies than the emission data because emission is more sensitive to temperature changes than absorption. In this regard, Figure 9 shows the marked change in the absorption spectra of the receptor with the addition of Trp, which can be associated with the formation of the supramolecular complex. By assuming that the static quenching is due the formation of a 1:1 complex between Trp and the acridine-based host molecule (A), the corresponding equilibrium is defined by Equation (4) and the equilibrium constant by Equation (5).

$$A + Trp \rightleftharpoons A\cdot Trp \quad (4)$$

$$K_S = [A\cdot Trp]/([A][Trp]) \quad (5)$$

The representation of ln$K$ versus $1/T$ (van't Hoff plot) allowed us to obtain the respective enthalpic and entropic parameters ΔH° and ΔS° involved in the binding process according to the expression of the Gibbs free energy of binding defined in Equation (6).[75]

$$\Delta G = \Delta H - T\Delta S = -RT\ln K_S \quad (6)$$

The variation of the absorbance in the titration of **1a** and **2a** with L-Trp at 5–35 °C in the UV/Vis titrations is displayed in Figure 12. It can be observed that the maximum variation of the absorbance decreases with the temperature and the curvature also follows the same trend, thus indicating that the complex formation is disfavored at higher temperatures. Moreover, both the maximum variation of the absorbance and the curvature are less marked in the open-chain compound **1a** relative to the macrocyclic compound **2a**, which clearly suggests that binding constants for macrocycle **2a** are larger than for **1a**, thus confirming the existence of a macrocyclic effect.[79,80]

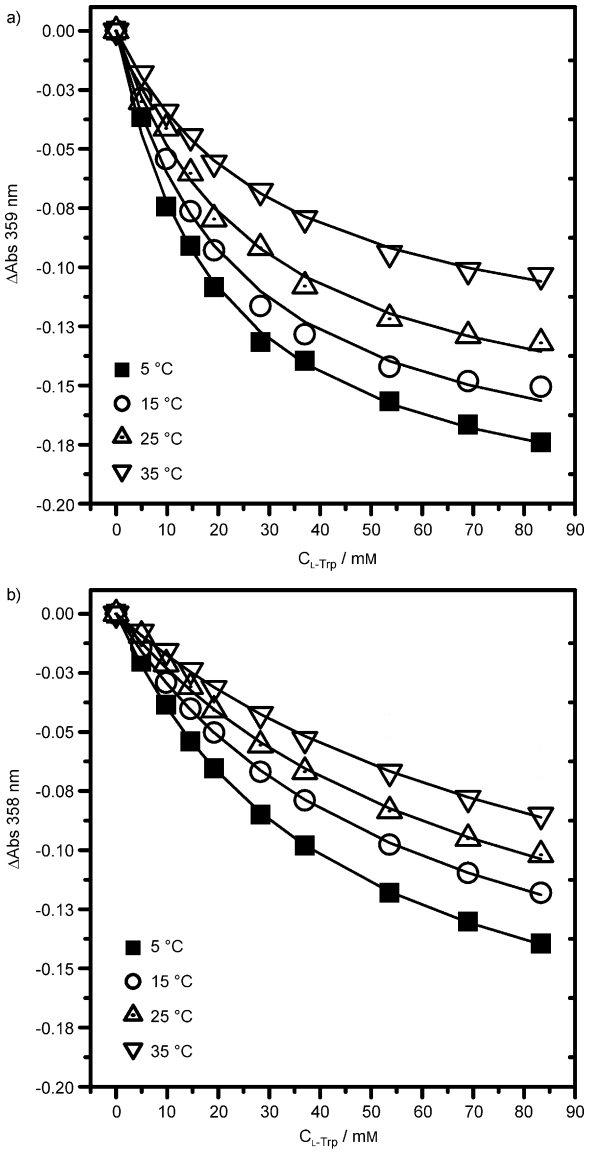

Figure 12. Variation of the Abs for the titration of: a) **1a** and b) **2a** (60 μM) with L-Trp (from 0 to 83 mM) in aqueous H_2SO_4 (1 M) at different temperatures (from 5 to 35 °C). Solid lines correspond to fitting to the 1:1 binding model.

A fitting for each titration to a 1:1 binding model was performed by using Equation (7),[81] where ΔAbs is the increment of the absorbance, ΔAbs_{max} is the maximum increment of the absorbance, c is the concentration of guest, c_0 is the concentration of the host, and K_S is the association constant (Figure 12). From the results obtained from the fitting at each temperature, the corresponding binding constants K_S were obtained (Table 4).

$$\Delta Abs = \Delta Abs_{max}/2(c/c_0 + 1 + 1/(K_S c_0) - \{[c/c_0 + 1 + 1/(K_S c_0)]^2 - 4c/c_0\}^{1/2}) \quad (7)$$

From the obtained binding constants, the corresponding van't Hoff representations were plotted (Figure 13). The data

Table 4. Parameters obtained from fitting to 1:1 Host–Guest model for the titration of **1a** and **2a** (60 μM) with L-Trp (from 0 to 83 mM) in aqueous H_2SO_4 (1 M).

T [°C]	K_S [M^{-1}] **1a**	K_S [M^{-1}] **2a**
5	23.2 ± 0.5	51 ± 3
15	17.4 ± 0.5	44 ± 4
25	13.6 ± 1.1	37 ± 4
35	10.7 ± 0.7	31.1 ± 1.6

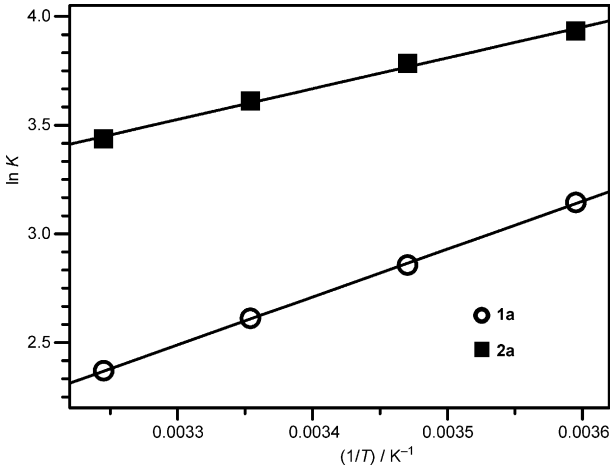

Figure 13. Variation of the ln$K$ with 1/T from fitting to the 1:1 host–guest model for the titration of **1a** and **2a** with L-Trp (from 0 to 83 mM) in aqueous H_2SO_4 (1 M). Probe concentration = 60 μM.

shows excellent linearity, and therefore it was possible to obtain the entropic and enthalpic contributions to the binding process (Table 5; note the small errors associated with each calculated thermodynamic parameter). In both compounds, the ΔS and ΔH values are negative. Despite the remarkable fact that the host and guest are positively charged these results confirm the presence of a significant enthalpic contribution that brings both molecules together. The unfavorable negative ΔS value can be rationalized in terms of the desolvation/solvation process during complex formation, thus leading to a host–guest complex more organized than the free molecules in solution. The comparison of the macrocyclic versus the open-chain structure is also interesting. On the one hand, the enthalpy contribution is more favorable (more negative) for the open-chain compound **1a** relative to the macrocyclic com-

Table 5. Parameters obtained from the fitting to a 1:1 Host–Guest model for the titration of **1a** and **2a** (60 μM) with L-Trp (from 0 to 83 mM) in aqueous H_2SO_4 (1 M).

[kal mol^{-1}]	**1a**	**2a**
ΔS	−9.5 ± 0.2	−2.3 ± 0.5
ΔH	−4.4 ± 0.1	−2.8 ± 0.1
$T\Delta S$ [a]	−2.8 ± 0.1	−0.7 ± 0.1
ΔG [a]	−1.5 ± 0.1	−2.1 ± 0.3

[a] Calculated at 298 K.

pound **2a**. This outcome is reasonable because the macrocyclic compound locates the three positive charges closer than in the open-chain compound **1a**, and the electrostatic repulsion is more difficult to avoid. But, on the other hand, the entropic contribution is more favorable (less negative) for macrocyclic compound **2a** as long as the macrocyclic compound is more preorganized and its conformation does not change upon complexation as much as the open-chain derivative **1a**. Overall, as a result of the combination of the former elements at 25 °C, the binding is more exergonic for the macrocyclic compound (-2.1 kcal mol^{-1}) than for the open-chain analogous derivative (-2.1 versus -1.5 kcal mol^{-1}, respectively).

As the supramolecular species considered involve the interaction of two positively charged entities, it is reasonable to assume that the counteranions present can have a significant effect and participate in the supramolecular species. Most of the checked anions provided some interference in the fluorescence experiments, but their effect on the binding constants could be studied by means of additional UV titration experiments of **2a** (60 μM) with L-Trp (0–83 mM) in different aqueous solutions of H_3PO_4, HCl, and HBr (1 M) at 5 °C. From fitting to a 1:1 host–guest model, the following binding constants were obtained: $K_S = 41 \pm 3$, 37.0 ± 1.0, and 21.5 ± 1.1 M^{-1} for HCl, HBr, and H_3PO_4, respectively. These binding constants confirm the involvement of the anions in the binding of both charged species and indicates that H_2SO_4 is best suited for the generation of the acidic media required for fluorescence sensing.

Computational models

Different computational calculations were carried out to postulate a tentative binding model. According to the experimental data, the HSO_4^- counterion must play an important role, most likely as a stabilizing element for the host–guest complex. Therefore, the computational calculations were carried out for the ternary complex formed between the receptor, Trp, and HSO_4^-. To make the calculations computationally accessible, the starting structures of the pseudopeptidic receptors were simplified and the pseudopeptidic structures **1c** and **2c** derived from alanine were used for the calculations (Figure 14).

Initially, different Monte Carlo conformational searches were performed with the Spartan '08 software[82] by using the MMFFaq force field. For each case, the most stable conformer obtained was fully optimized by using the Gaussian 09 software at the PM6 level of theory with water as the solvent.[83] In these simulations, the amine groups of the pseudopeptides were fully protonated to simulate the acidic pH values at which the experiments were carried out. In the absence of hydrogen sulfate counteranions, it was not possible to obtain a minimized supramolecular complex due to the electrostatic repulsion between the two cationic species. In contrast, when four hydrogen sulfate counteranions were included in the simulation to counterbalance the positive charge of the protonated host and guest, it was possible to optimize the structure of the supramolecular complex, thus obtaining the geometry of the supramolecular complexes displayed in Figure 15. In such complexes, the distances between the center of the indole ring of Trp and the center of the acridine ring of the pseudopeptide are 4.46 and 4.48 Å (MMFFaq and PM6, respectively; solvent = water) for **1c** and 4.17 and 4.20 Å (MMFFaq and PM6, respectively; solvent = water) for **2c**. Although this model can be considered to be very simplistic, the obtained structures for the complexes are in good agreement with the experimental observations and show how aromatic interactions between the acridinium and indole rings are possible and can be responsible for the strong fluorescence quenching observed in the presence of Trp and for the selectivity observed for this amino acid.

Alternatively, optimizations in the presence of explicit water molecules allowed us to minimize the supramolecular complex

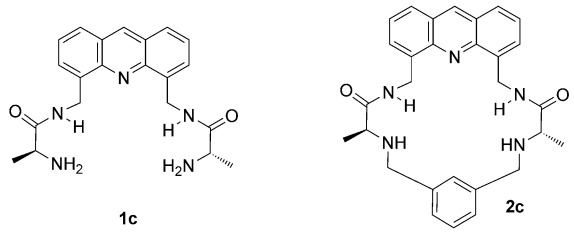

Figure 14. The pseudopeptidic structures used for the computational calculations.

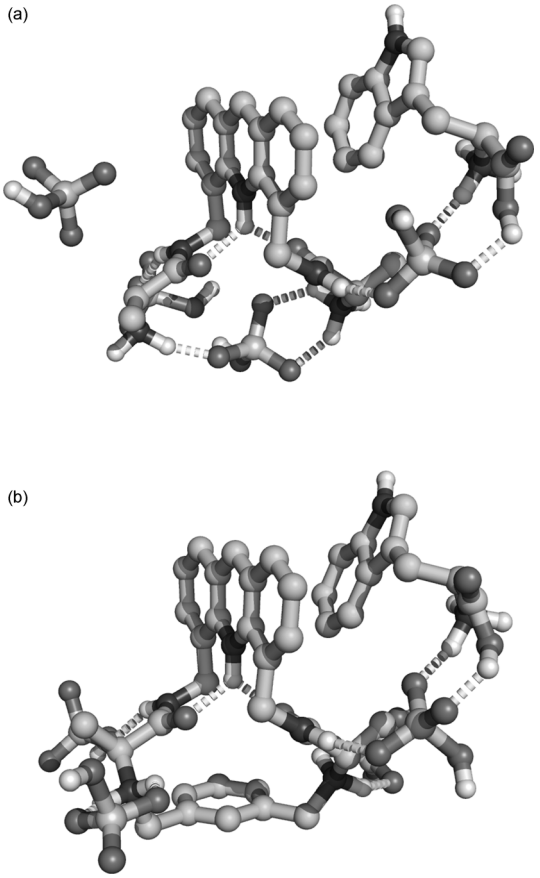

Figure 15. Optimized geometries (PM6, solvent = water) for the complexes with L-Trp in the presence of 4 HSO_4^- counteranions and receptors **1c** (a) and **2c** (b).

in the presence and absence of any counteranion (see the Supporting Information). The calculated structures show that in the absence of the corresponding counteranions formation of the supramolecular complex forces the existence of stronger π–π interactions. Very interestingly, there is a good agreement between the structures calculated by both methodologies when the four couteranions are present. Thus, the distances between the center of the indole ring of Trp and the center of the acridine ring of the pseudopeptide in the presence of 4 HSO_4^- counteranions are 4.65 and 4.10 Å for **1c** and **2c**, respectively; however, in the absence of counteranions, those distances are 3.84 and 3.87 Å, respectively.

Additional evidence for the participation of this type of supramolecular species, according to the former model, was provided by DOSY NMR spectroscopic experiments. The diffusion coefficients for **2a** in the absence and presence of L-Trp were measured. The measurements were carried out in 5 M H_2SO_4 in D_2O with tetraethylammonium (5 mM) as the internal standard. The concentrations of the guest and host were 10 and 50 mM for **2a** and L-Trp, respectively, to ensure that about 60% of the complex is formed (according to the calculated constants). From the obtained diffusion coefficients (i.e., $D(\mathbf{2a}+\text{L-Trp}) = (1.10 \pm 0.03)\cdot 10^{-10}$ and $D(\mathbf{2a}) = (1.28 \pm 0.05)\cdot 10^{-10}$ $m^2 s^{-1}$ as the average of four different experiments), the hydrodynamic radius was obtained by using the Stokes–Einstein equation $R = kT/(6\pi\eta D)$: $R(\mathbf{2a}+\text{L-Trp}) = (8.25 \pm 0.37)$ and $R(\mathbf{2a}) = (7.36 \pm 0.30)$ Å. The agreement of these data with the computational models can be considered to be good. For the structures computed by using a continuous solvation model, the calculated radii of the spheres with origins in the center of mass that include all atoms (Figure 16; i.e., $R_{max}(\mathbf{2a}+\text{L-Trp}) = 8.88$ and $R_{max}(\mathbf{2a}) = 7.67$ Å) are only slightly larger than those obtained experimentally. This outcome is to be expected taking into consideration that only approximately 60% of the complex is formed under the experimental conditions used. In fact, the computed ratio of $R_{max}(\mathbf{2a}+\text{L-Trp})/R_{max}(\mathbf{2a})$ is 1:1.16, whereas the experimentally obtained ratio of $R(\mathbf{2a}+\text{L-Trp})/R(\mathbf{2a})$ is $1:1.120 \pm 0.011$.[84] For the models calculated in the presence of explicit water molecules, some interesting data can be obtained. When the presence of the counteranions is also considered explicitly, the results show an excellent agreement with those obtained by using the continuum model and those obtained from DOSY experiments, with $R_{max}(\mathbf{2a}+\text{L-Trp}) = 9.33$ and $R_{max}(\mathbf{2a}) = 7.99$ Å. Some overestimation of the R_{max} values is observed, which, in the case of the complex, could be assignable to partial complex formation, but the value obtained for the R_{max} ratio (1:1.17) is again very close to the experimental value, as mentioned above. In the absence of HSO_4^- ions, however, the calculated values are $R_{max}(\mathbf{2a}+\text{L-Trp}) = 7.93$ and $R_{max}(\mathbf{2a}) = 6.13$ Å, and the R_{max} ratio is 1:1.29, which are much less consistent with the experimental values. These experiments, along with the observed influence of the nature of the anion present, strongly suggest the involvement of the counteranions in the supramolecular species. The participation of anions in the assembly of two species with the same charge assisted by anions suggested in our model is similar to those described by the counterion-condensation theory of attraction between like charges assisted by counterions.[85–87]

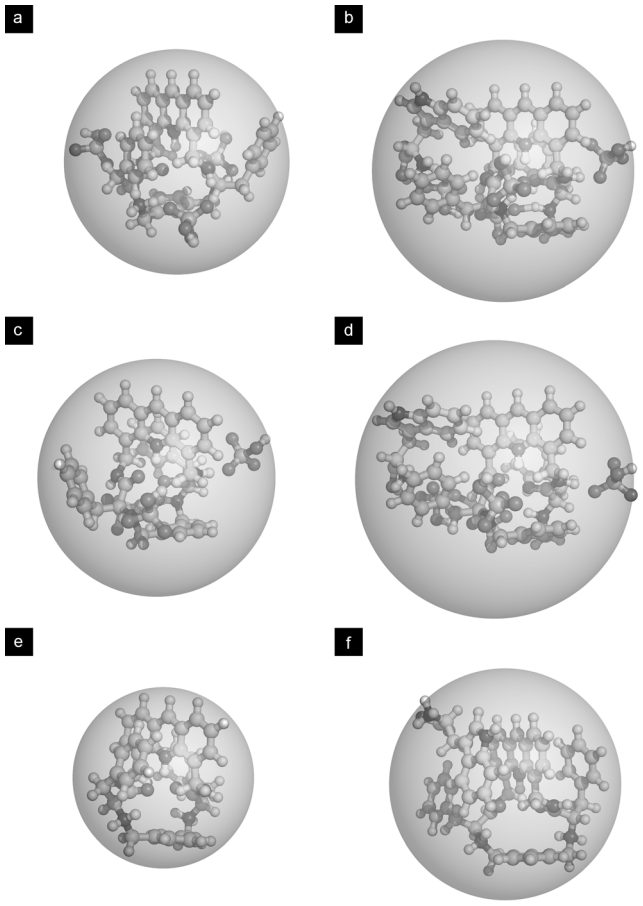

Figure 16. R_{max} values for the optimized geometries (MMFFaq): a) $H_3\mathbf{2a}^{3+}$ in the presence of 3 HSO_4^- counteranions ($R_{max}(\mathbf{2a}) = 7.67$ Å); b) the complex of $H_3\mathbf{2a}^{3+}$ with L-Trp–H_2^+ in the presence of 4 HSO_4^- counteranions ($R_{max} = 8.88$ Å); c) $H_3\mathbf{2a}^{3+}$ in the presence of 3 HSO_4^- counteranions with explicit water molecules ($R_{max} = 7.99$ Å); d) the complex of $H_3\mathbf{2a}^{3+}$ with L-Trp–H_2^+ in the presence of 4 HSO_4^- counteranions with explicit water molecules ($R_{max} = 9.33$ Å); e) $H_3\mathbf{2a}^{3+}$ with explicit water molecules ($R_{max} = 6.13$ Å); f) the complex of $H_3\mathbf{2a}^{3+}$ with L-Trp-H_2^+ with explicit water molecules ($R_{max} = 7.93$ Å).

Conclusion

Two new pseudopeptidic receptors derived from valine (open-chain and macrocyclic) and containing an acridine spacer have been designed, synthesized, and characterized. Both receptors and the previously prepared phenylalanine-derived compounds can associate with free tryptophan in 100% aqueous medium under very acidic conditions. Other studied amino acids show low (Tyr) or negligible (Met, His, Phe, Val, Ala) complexation. Macrocyclic compounds bound more efficiently to Trp than the related open-chain compounds, most likely because of their more favorable preorganization. The recognition process was studied using ^{1}H NMR, UV/Vis, and fluorescence spectroscopic analysis and computational calculations, and

a good agreement between all the data was observed. Very interestingly, the results reported herein clearly highlight the association between two positively charged species, in which the interaction involves aromatic interactions and, most likely, electrostatic and hydrogen-bonding interactions that involve the counteranions and solvent molecules. This strong interaction between the indole ring of the tryptophan and the acridinium ring of the host seems to be responsible for the selectivity observed for this amino acid. A direct extrapolation of our results to the biological realm is not possible due to the non-natural very acidic conditions required for our experiments. However, the results obtained illustrate the potential to establish supramolecular species between two positively charged species, in particular when assisted by the proper counteranions, which can be of interest for understanding different association processes of biological relevance. Thus, the formation of a supramolecular complex needs to involve strong favorable interactions to compensate for this initial electrostatic repulsion.

On the other hand, as the selective recognition process of tryptophan is associated with strong quenching of the fluorescence of the acridinium subunit at the receptor, the present results open new approaches for the development of fluorescent selective sensors for an important biological target, such as the amino acid tryptophan.

Experimental Section

Materials and methods

All the commercially available reagents and solvents were used as received, without further purification. Acridine was recrystallized from ethanol/water as described previously.[66]

Steady-state fluorescence spectroscopy: For fluorescence titrations in water, steady-state fluorescence spectra were recorded on a Spex Fluorolog 3–11 fluorimeter equipped with a 450 W xenon lamp. Fluorescence spectra were recorded in the front-face mode.

Time-resolved fluorescence spectroscopy: Time-resolved fluorescence measurements were carried out by using time-correlated single-photon counting (TCSPC) on an IBM-5000J apparatus. Samples were excited with a NanoLED at $\lambda = 372$ nm with a full width at half maximum (FWHM) value of $\lambda = 1.3$ ns and a repetition rate of 100 kHz. Data were fitted to the appropriate exponential model after deconvolution of the instrument response function by using an iterative deconvolution technique with the IBH DAS6 fluorescence-decay-analysis software, in which reduced χ^2 and weighted residuals serve as parameters for the goodness of fit.

NMR spectroscopy: ^{1}H and ^{13}C NMR spectra were recorded on a 500 MHz spectrometer (500 and 125 MHz for ^{1}H and ^{13}C, respectively) or a 300 MHz spectrometer (300 and 75 MHz for ^{1}H and ^{13}C, respectively).

IR spectroscopy: Attenuated total reflectance (ATR) FTIR spectra were acquired on a JASCO 6200 equipment with a MIRacle single-reflection ATR diamond/ZnSe accessory. The raw IR data were processed with the JASCO spectral manager software.

UV/Vis spectroscopy: UV/Vis absorption measurements were recorded on a Hewlett–Packard 8453 spectrophotometer, equipped with a temperature-control accessory Peltier Agilent 89090A.

Fluorescence measurements

Titrations with amino acids in water: The compounds were dissolved in 1 M H_2SO_4 to obtain 1 mM stock solutions from which 20 μM solutions in 1 M H_2SO_4 were prepared. These solutions were titrated by adding increasing volumes of stock solutions of 0–36 mM of the corresponding amino acids in 1 M H_2SO_4.

pH titrations in water: The different compounds were dissolved in dimethyl sulfoxide (DMSO) to obtain 1 mM stock solutions. Those solutions were diluted to 10 μM with water containing a mixture of several buffers to facilitate titrations between pH 9 and 1 (sodium acetate (40 mM), sodium phosphate (40 mM), sodium borate (40 mM), and sodium carbonate (40 mM)). A small final percentage of DMSO (1–2%) was required to avoid the precipitation of the compounds due to their low solubility in water. Slight variations in the pH values of the solutions were achieved by adding the minimum volumes of 0.1–1.0 M NaOH or 0.1–1.0 M HCl (typically 10 μL added to 10 mL), in such a way that dilution effects were negligible. The pK_a values were obtained from the nonlinear curve-fitting of the data with Origin 6.1.

Fluorescence-lifetime determination: Compounds were dissolved in water and H_2SO_4 to obtain stock solutions (1 mM). These solutions were diluted to 20 μM with water. Variations in the pH value of the solutions were achieved by adding H_2SO_4 or NaOH. The samples were purged with nitrogen.

Quantum-yield determination: Solutions of the compounds were prepared as described for the fluorescence-lifetime determination. Fluorescence quantum yields of **1**, **2**, and acridine are reported relative to quinine sulphate (aqueous solution in 0.1 M H_2SO_4, air) with $\Phi_F = 0.53$.[67] The experiments were carried out in optically matching solutions. Emission spectra were recorded upon excitation at $\lambda_{exc} = 366$ nm. The quantum yield was calculated by using Equation (8). In this expression, it is assumed that the sample and the reference are excited at the same wavelength so that it is not necessary to correct for the different excitation intensities at different wavelengths.

$$\Phi_f = \Phi_r \times (A_r F_s / A_s F_r) \times (n_s^2 / n_r^2) \quad (8)$$

where Φ_f is the quantum yield, F is the integrated intensity, A is the optical density, and n is the refractive index. The subscript r refers to the reference fluorophore of known quantum yield and subscript s to the sample. The spectra were appropriately corrected.

NMR diffusion studies

All DOSY experiments were conducted in quadruplicate on a Varian NMR System 500 MHz spectrometer at 300 K equipped with PERFORMA IV pulse-field gradients. Data were collected with the bipolar pulse-pair stimulated-echo sequence. The diffusion parameters were optimized to obtain a 90–95% on signal-intensity decay. Typical values are diffusion times (Δ) of 100 ms, with encoding gradient pulses of total a duration δ of 2 ms. An array of 30 values of gradient strength was acquired with 14 scans per value. Diffusion coefficients were calculated by using the values of the intensity of the observed signal from the Stejskal–Tanner equation[88] with Origin 6.1 software.

Computational studies

Monte Carlo conformational searches with the MMFFaq force field were carried out with the Spartan '08 software for triprotonated model compounds **1c** and **2c**[82] and their supramolecular com-

plexes with monoprotonated tryptophan in the presence and absence of hydrogen sulfate counteranions. The most stable conformers were optimized at the PM6 level of theory with water as the solvent in the Gaussian 09 software.[83] All the geometries were fully optimized and were checked to be true minima by analysis of the vibration normal modes. The **2a** model employed for the calculation of the R_{max} value was obtained from the **2c** MMFFaq most stable conformers by adding the phenyl substituents. Explicit water molecules were added by using the solvate plugin (TIP3BOX solvent model, the box salvation model, and a box size of 5) implemented in the UCSF Chimera package and the resulting solvated structure was minimized with the Spartan '08 software. Chimera was developed by the Resource for Biocomputing, Visualization, and Informatics at the University of California (San Francisco, USA; supported by NIGMS P41-GM103311).[89]

Synthesis of receptors

Compound 1b-Cbz: Aqueous NaOH (1 M, 10 mL) and MeOH (1 mL) were added to 4,5-bis(aminomethyl)acridine·2HCl (0.200 g, 0.645 mmol) placed in a 50 mL round-bottom flask. After complete dissolution of the solid, the solution was extracted three times with dichloromethane (15 mL). The organic layers were collected and dried over anhydrous $MgSO_4$. The solvent was then vacuum evaporated to afford 4,5-bis(aminomethyl)acridine (0.142 g, 0.600 mmol, 93%) as a yellowish solid. This solid was dissolved in DME (15 mL) in a 50 mL round-bottom flask. Cbz-L-Val-OSu (0.418 g, 1.2 mmol) was dissolved in DME (10 mL) and slowly added to the reaction flask. A white precipitate was rapidly formed and the mixture was stirred at room temperature for 20 h and then at 50 °C for 6 h. After cooling, a white precipitate was collected by filtration and washed with cold water (50 mL) and a small amount of methanol to afford the expected compound **1b-Cbz** as a white solid (0.266 g, 0.378 mmol, 63%). M.p. 252–255 °C; $[\alpha]_D^{25} = 13.94^\circ$ ($c = 0.01$ in DMSO); ^{1}H NMR (500 MHz, [D$_6$]DMSO): $\delta = 9.10$ (s, 1H), 8.50 (t, 2H, $J = 5.7$ Hz), 8.06 (d, ^3J(H,H) = 8.4 Hz, 2H), 7.71 (d, ^3J(H,H) = 6.7 Hz, 2H), 7.47–7.61 (m, 2H), 7.33 (d, ^3J(H,H) = 4.5 Hz, 12H), 4.72–5.42 (m, 8H), 3.97 (t, ^3J(H,H) = 7.9 Hz, 2H), 2.02 (dd, ^3J(H,H) = 6.9, 13.5 Hz, 2H), 0.80–1.01 ppm (m, 12H); ^{13}C NMR (75 MHz, [D$_6$]DMSO): $\delta = 172.2$, 156.9, 146.3, 137.8, 137.4, 129.0, 128.4, 128.3, 128.3, 127.9, 126.6, 126.3, 126.2, 66.1, 61.3, 39.4, 30.8, 20.0, 18.9 ppm; IR (ATR) $\tilde{\nu} = 1454$, 1645, 3064, 3282 cm^{-1}; HRMS (ESI-TOF): *m/z* calcd for $C_{41}H_{45}N_5O_6$: 704.3448 [$M+H^+$]; found 704.3458; elemental analysis calcd (%) for $C_{41}H_{45}N_5O_6$: C 69.97, H 6.44, N 9.95; found: C 69.86, H 6.48, N 10.12.

Compound 1b: A HBr/AcOH solution (33%, 50 mL) was added to **1b-Cbz** (2.000 g, 2.84 mmol) placed into a 100 mL round-bottom flask. After complete dissolution of the solid, a yellow solution was formed. The reaction was stirred in a nitrogen atmosphere for 1 h. The resulting colorless solution was poured into a 250 mL beaker containing diethyl ether (150 mL). A white precipitate was collected by filtration and washed with diethyl ether. The solid was redissolved in distilled water (30 mL), the solution was washed twice with $CHCl_3$ (30 mL), and was basified with solid NaOH until pH 12–13. NaCl was added until saturation and the aqueous phase was extracted three times with $CHCl_3$ (30 mL). The organic phase was dried over anhydrous $MgSO_4$, and the solvent was eliminated by vacuum to afford **1** as a white solid (1.014 g, 2.329 mmol, 82%). M.p. 126 °C; $[\alpha]_D^{25} = -73.60^\circ$ ($c = 0.01$ in $CHCl_3$); ^{1}H NMR (500 MHz, $CDCl_3$): $\delta = 8.71$ (s, 1H), 8.55 (s, 2H), 7.87 (2H, d, ^3J(H,H) = 8.5 Hz), 7.74 (d, ^3J(H,H) = 6.7 Hz, 2H), 7.43 (t, ^3J(H,H) = 7.5 Hz, 2H), 5.17 (qd, ^3J(H,H) = 6.2, 14.5 Hz, 4H), 3.20 (d, ^3J(H,H) = 3.4 Hz, 2H), 2.23 (dd, ^3J(H,H) = 6.5, 10.6 Hz, 2H), 1.37 (s, 4H), 0.86 (d, ^3J(H,H) = 6.9 Hz, 6H), 0.69 ppm (d, ^3J(H,H) = 6.8 Hz, 6H); ^{13}C NMR (126 MHz, $CDCl_3$): $\delta =$ 174.3, 146.8, 136.7, 136.4, 129.5, 127.7, 126.6, 125.7, 60.4, 40.6, 30.9, 19.7, 16.1 ppm; IR (ATR): $\tilde{\nu} = 1430$, 1638, 3066, 3277 cm^{-1}; HRMS (ESI-TOF): *m/z* calcd for $C_{41}H_{39}N_5O_2$: 436.2713 [$M+H^+$]; found 436.2717; elemental analysis calcd (%) for $C_{41}H_{39}N_5O_2$: C 68.94, H 7.64, N 16.08; found: C 68.82, H 7.62 N, 15.82.

Compound 2b: Dry acetonitrile (165 mL) was added to **1b** (0.500 g, 1.148 mmol), TBABr (0.1850 g, 0.574 mmol), and DIPEA (1.965 mL, 11.48 mmol) placed in a 250 mL round-bottom flask. The reaction mixture was stirred at room temperature until complete dissolution of the reagents, and then 1,3-bis(bromomethyl)-benzene (0.3030 g, 1.148 mmol) dissolved in a small amount of dry acetonitrile was added. The reaction mixture was heated using a temperature gradient from 50.0 to 81.6 °C (to reflux) for 24 h in a nitrogen atmosphere. After cooling, the solvent was eliminated by vacuum. Purification of the crude product was carried out by column chromatography over silica gel (dichloromethane/methanol 100:0→100:5 with a few drops of aqueous ammonia). The macrocycle was obtained as a white solid (0.3889 g, 0.723 mmol, 63%). M.p. 100–102 °C; $[\alpha]_D^{25} = 103.98$ ($c = 0.01$ in $CHCl_3$); ^{1}H NMR (500 MHz, $CDCl_3$): $\delta = 8.67$ (s, 1H), 8.13 (d, ^3J(H,H) = 5.7 Hz, 2H), 7.84 (d, ^3J(H,H) = 8.4 Hz, 2H), 7.73 (d, ^3J(H,H) = 6.6 Hz, 2H), 7.42 (t, ^3J(H,H) = 7.5 Hz, 2H), 7.31 (s, 1H), 7.05–7.19 (m, 3H), 5.10 (dd, ^3J(H,H) = 7.9, 14.9 Hz, 2H), 4.78 (dd, ^3J(H,H) = 5.0, 14.9 Hz, 2H), 3.96 (d, ^3J(H,H) = 12.6 Hz, 2H), 3.54 (d, ^3J(H,H) = 12.6 Hz, 2H), 3.01 (d, ^3J(H,H) = 4.6 Hz, 2H), 1.98 (dd, ^3J(H,H) = 6.4, 11.9 Hz, 4H), 0.85 (d, ^3J(H,H) = 6.9 Hz, 6H), 0.68 ppm (d, ^3J(H,H) = 6.8 Hz, 6H); ^{13}C NMR (126 MHz, $CDCl_3$): $\delta = 174.0$, 146.6, 140.4, 136.7, 136.4, 129.2, 129.1, 128.9, 127.6, 127.6, 126.4, 125.6, 69.8, 54.4, 40.6, 31.5, 19.6, 17.9 ppm; IR (ATR): $\tilde{\nu} = 3290$, 2870, 1646, 1387, 1555, 1513 cm^{-1}; HRMS (ESI-TOF): *m/z* calcd for $C_{33}H_{39}N_5O_2$: 538.3181 [$M+H^+$]; found: 538.3180; elemental analysis calcd (%) for $C_{33}H_{39}N_5O_2$: C 73.71, H 7.31, N 13.02; found: C 73.47, H 7.37, N 12.79.

Acknowledgements

Financial support from was provided by the Spanish MINECO (CTQ2012-38543-C03-01) and Generalitat Valenciana (PROMETEO 2012/020). V.M.-C acknowledges the Spanish Ministry of Science (FPU AP2007-02562) and Generalitat Valenciana (APOSTD/2013/041) for personal support. The technical support of the SCIC of the UJI for different instrumental techniques is acknowledged.

Keywords: fluorescence · molecular recognition · pseudopeptides · supramolecular chemistry · tryptophan

[1] O. Keskin, A. Gursoy, B. Ma, R. Nussinov, *Chem. Rev.* **2008**, *108*, 1225–1244.
[2] P. A. Gale, *Chem. Soc. Rev.* **2007**, *36*, 141–142.
[3] P. D. Beer, P. Schmitt, *Curr. Opin. Chem. Biol.* **1997**, *1*, 475–482.
[4] A. S. DeToma, S. Salamekh, A. Ramamoorthy, M. H. Lim, *Chem. Soc. Rev.* **2012**, *41*, 608–621.
[5] P. A. Gale, J. W. Steed, *Supramolecular Chemistry: From Molecules to Nanomaterial: Molecular Recognition, Vol. 3,* Wiley, Hoboken, **2012**.
[6] P. A. Gale, *Chem. Commun.* **2011**, *47*, 82–86.
[7] P. A. Gale, S. E. García-Garrido, J. Garric, *Chem. Soc. Rev.* **2008**, *37*, 151–190.
[8] P. D. Beer, P. A. Gale, *Angew. Chem.* **2001**, *113*, 502–532; *Angew. Chem. Int. Ed.* **2001**, *40*, 486–516.
[9] K. M. Mullen, P. D. Beer, *Chem. Soc. Rev.* **2009**, *38*, 1701–1713.
[10] F. Zapata, A. Caballero, N. G. White, T. D. W. Claridge, P. J. Costa, V. t. Félix, P. D. Beer, *J. Am. Chem. Soc.* **2012**, *134*, 11533–11541.

[11] B. Wang, E. V. Anslyn, *Chemosensors: Principles, Strategies, and Applications*, Wiley, Hoboken, **2011**.
[12] S. Kubik, *Chem. Soc. Rev.* **2010**, *39*, 3648 – 3663.
[13] S. Kubik, C. Reyheller, S. Stüwe, *J. Incl. Phenom.* **2005**, *52*, 137 – 187.
[14] P. A. Gale, *Chem. Soc. Rev.* **2010**, *39*, 3746 – 3771.
[15] S. V. Luis, I. Alfonso, F. Galindo in *Supramolecular Chemistry: From Molecules to Nanomaterials. Vol. 3: Molecular Recognition*, (Eds.: P. Gale, J. Steed), Wiley, Chichester, **2012**.
[16] Y. Zhou, J. Yoon, *Chem. Soc. Rev.* **2012**, *41*, 52 – 67.
[17] C.-S. Lee, P.-F. Teng, W.-L. Wong, H.-L. Kwong, A. S. C. Chan, *Tetrahedron* **2005**, *61*, 7924 – 7930.
[18] J. F. Folmer-Andersen, M. Kitamura, E. V. Anslyn, *J. Am. Chem. Soc.* **2006**, *128*, 5652 – 5653.
[19] D. Leung, J. F. Folmer-Andersen, V. M. Lynch, E. V. Anslyn, *J. Am. Chem. Soc.* **2008**, *130*, 12318 – 12327.
[20] L. Fabbrizzi, M. Licchelli, A. Perotti, A. Poggi, G. Rabaioli, D. Sacchi, A. Taglietti, *J. Chem. Soc. Perkin Trans. 2* **2001**, 2108 – 2113.
[21] F. Galindo, J. Becerril, M. I. Burguete, S. V. Luis, L. Vigara, *Tetrahedron Lett.* **2004**, *45*, 1659 – 1662.
[22] M. I. Burguete, G. Fawaz, F. Galindo, M. A. Izquierdo, S. V. Luis, J. Martínez, X. J. Salom-Roig, *Tetrahedron* **2009**, *65*, 7801 – 7808.
[23] M. I. Burguete, F. Galindo, S. V. Luis, L. Vigara, *J. Photochem. Photobiol. A* **2010**, *209*, 61 – 67.
[24] X. Mei, C. Wolf, *J. Am. Chem. Soc.* **2004**, *126*, 14736 – 14737.
[25] L. Mutihac, J. H. Lee, J. S. Kim, J. Vicens, *Chem. Soc. Rev.* **2011**, *40*, 2777 – 2796.
[26] R. Joseph, J. P. Chinta, C. P. Rao, *J. Org. Chem.* **2010**, *75*, 3387 – 3395.
[27] Y. Willener, K. M. Joly, C. J. Moody, J. H. R. Tucker, *J. Org. Chem.* **2008**, *73*, 1225 – 1233.
[28] S. Shinoda, T. Okazaki, T. N. Player, H. Misaki, K. Hori, H. Tsukube, *J. Org. Chem.* **2005**, *70*, 1835 – 1843.
[29] F. Wang, A. W. Schwabacher, *J. Org. Chem.* **1999**, *64*, 8922 – 8928.
[30] M. Hariharan, S. C. Karunakaran, D. Ramaiah, *Org. Lett.* **2007**, *9*, 417 – 420.
[31] E. M. Goldys, *Fluorescence Applications in Biotechnology and Life Sciences,* Wiley, Hoboken, **2009**.
[32] H. Neuweiler, A. Schulz, A. C. Vaiana, J. C. Smith, S. Kaul, J. Wolfrum, M. Sauer, *Angew. Chem.* **2002**, *114*, 4964 – 4968; *Angew. Chem. Int. Ed.* **2002**, *41*, 4769 – 4773.
[33] M. Götz, S. Hess, G. Beste, A. Skerra, M. E. Michel-Beyerle, *Biochemistry* **2002**, *41*, 4156 – 4164.
[34] H. Chen, S. S. Ahsan, M. B. Santiago-Berrios, H. D. Abruña, W. W. Webb, *J. Am. Chem. Soc.* **2010**, *132*, 7244 – 7245.
[35] M. Hossain, H. J. Schneider, *J. Am. Chem. Soc.* **1998**, *120*, 11208 – 11209.
[36] J. Rebek, B. Askew, D. Nemeth, K. Parris, *J. Am. Chem. Soc.* **1987**, *109*, 2432 – 2434.
[37] M. Fokkens, T. Schrader, F.-G. Klärner, *J. Am. Chem. Soc.* **2005**, *127*, 14415 – 14421.
[38] N. Marmé, J. P. Knemeyer, M. Sauer, J. Wolfrum, *Bioconjugate Chem.* **2003**, *14*, 1133 – 1139.
[39] A. C. Vaiana, H. Neuweiler, A. Schulz, J. Wolfrum, M. Sauer, J. C. Smith, *J. Am. Chem. Soc.* **2003**, *125*, 14564 – 14572.
[40] S. Doose, H. Neuweiler, M. Sauer, *ChemPhysChem* **2005**, *6*, 2277 – 2285.
[41] L. Yang, S. Qin, X. Su, F. Yang, J. You, C. Hu, R. Xie, J. Lan, *Org. Biomol. Chem.* **2010**, *8*, 339 – 348.
[42] J. R. Moffett, M. Namboodiri, *Immunol. Cell Biol.* **2003**, *81*, 247 – 265.
[43] G. M. Mackay, C. M. Forrest, N. Stoy, J. Christofides, M. Egerton, T. W. Stone, L. G. Darlington, *Eur. J. Neurol.* **2006**, *13*, 30 – 42.
[44] A. Slominski, I. Semak, A. Pisarchik, T. Sweatman, A. Szczesniewski, J. Wortsman, *FEBS Lett.* **2002**, *511*, 102 – 106.
[45] S. V. Luis, I. Alfonso, *Acc. Chem. Res.* **2014**, *47*, 112 – 124
[46] K. Kano, H. Minamizono, T. Kitae, S. Negi, *J. Phys. Chem. A* **1997**, *101*, 6118 – 6124.
[47] V. Martí-Centelles, M. I. Burguete, F. Galindo, M. A. Izquierdo, D. K. Kumar, A. J. P. White, S. V. Luis, R. Vilar, *J. Org. Chem.* **2012**, *77*, 490 – 500.
[48] D. G. Carole, D. M. Michel, C. Julien, D. Florence, N. Anna, J. Séverine, D. Gérard, T. D. Pierre, G. Jean-Pierre, *Bioorg. Med. Chem.* **2005**, *13*, 5560 – 5568.
[49] F. Hess, E. Cullen, K. Grozinger, *Tetrahedron Lett.* **1971**, *12*, 2591 – 2594.
[50] F. K. Hess, P. B. Stewart, *J. Med. Chem.* **1975**, *18*, 320 – 321.
[51] M. Laronze-Cochard, Y. M. Kim, B. Brassart, J. F. Riou, J. Y. Laronze, J. Sapi, *Eur. J. Med. Chem.* **2009**, *44*, 3880 – 3888.
[52] K. Omata, M. Hashimoto, Sutarto, M. Yamada, *Ind. Eng. Chem. Res.* **2009**, *48*, 844 – 849.
[53] D. Parker, *Macrocycle Synthesis: A Practical Approach*, Oxford University Press, Oxford, **1996**.
[54] S. E. Gibson, C. Lecci, *Angew. Chem.* **2006**, *118*, 1392 – 1405; *Angew. Chem. Int. Ed.* **2006**, *45*, 1364 – 1377.
[55] V. Martí-Centelles, M. I. Burguete, S. V. Luis, *Chem. Eur. J.* **2012**, *18*, 2409 – 2422.
[56] V. Martí-Centelles, M. I. Burguete, S. V. Luis, The Scientific World Journal Volume 2012 (2012), Article ID 748251, 14 pages http://dx.doi.org/10.1100/2012/748251.
[57] J. Becerril, M. Bolte, M. I. Burguete, F. Galindo, E. García-España, S. V. Luis, J. F. Miravet, *J. Am. Chem. Soc.* **2003**, *125*, 6677 – 6686.
[58] M. I. Burguete, F. Galindo, M. A. Izquierdo, S. V. Luis, L. Vigara, *Tetrahedron* **2007**, *63*, 9493 – 9501.
[59] M. I. Burguete, F. Galindo, M. A. Izquierdo, J. E. O'Connor, G. Herrera, S. V. Luis, L. Vigara, *Eur. J. Org. Chem.* **2010**, 5967 – 5979.
[60] F. Galindo, M. I. Burguete, L. Vigara, S. V. Luis, N. Kabir, J. Gavrilovic, D. A. Russell, *Angew. Chem.* **2005**, *117*, 6662 – 6666; *Angew. Chem. Int. Ed.* **2005**, *44*, 6504 – 6508.
[61] F. Huang, W. M. Nau, *Angew. Chem.* **2003**, *115*, 2371 – 2374; *Angew. Chem. Int. Ed.* **2003**, *42*, 2269 – 2272.
[62] S. L. Murov, *Handbook of Photochemistry,* Marcel Dekker, New York, **1973**.
[63] Y. Huh, J.-G. Lee, D. C. McPhail, K. Kim, *J. Solution Chem.* **1993**, *22*, 651 – 661.
[64] L. A. Diverdi, M. R. Topp, *J. Phys. Chem.* **1984**, *88*, 3447 – 3451.
[65] K. Kasama, K. Kikuchi, Y. Nishida, H. Kokubun, *J. Phys. Chem.* **1981**, *85*, 4148 – 4153.
[66] K. Kasama, K. Kikuchi, S. A. Yamamoto, K. Uji-ie, Y. Nishida, H. Kokubun, *J. Phys. Chem.* **1981**, *85*, 1291 – 1296.
[67] M. J. Adams, J. G. Highfield, G. F. Kirkbright, *Anal. Chem.* **1977**, *49*, 1850 – 1852.
[68] J. Aguilar, M. G. Basallote, L. Gil, J. C. Hernandez, M. A. Manez, E. Garcia-España, C. Soriano, B. Verdejo, *Dalton Trans.* **2004**, 94 – 103.
[69] I. Alfonso, M. Bolte, M. Bru, M. I. Burguete, S. V. Luis, C. Vicent, *Org. Biomol. Chem.* **2010**, *8*, 1329 – 1339.
[70] J. R. Lakowicz, *Principles of Fluorescence Spectroscopy* 2nd Ed., Springer, New York, **2006**.
[71] F. Galindo, M. C. Jimenez, M. A. Miranda, R. Tormos, *Chem. Commun.* **2000**, 1747 – 1748.
[72] A. M. Amat, A. Arques, F. Galindo, M. A. Miranda, L. Santos-Juanes, R. F. Vercher, R. Vicente, *Appl. Catal. B* **2007**, *73*, 220 – 226.
[73] B. S. Andonovski, *Croat. Chem. Acta* **1999**, *72*, 711 – 726.
[74] E. Canel, A. Gültepe, A. Doğan, E. Kilıç, *J. Solution Chem.* **2006**, *35*, 5 – 19.
[75] J. W. Steed, J. L. Atwood, *Supramolecular Chemistry,* Wiley, Chichester, **2009**.
[76] A. Rice, *Comprehensive Chemical Kinetics, Vol. 25, Diffusion Limited Reactions*, Elsevier, New York, **1985**.
[77] T. Pedzinski, B. Marciniak, G. L. Hug, *J. Photochem. Photobiol. A* **2002**, *150*, 21 – 30.
[78] D. Rehm, A. Weller, *Chemie Z. Phys. Chem.* **1970**, *69*, 183 – 200.
[79] J. N. Spencer, J. E. Mihalick, T. J. Nicholson, P. A. Cortina, J. L. Rinehimer, J. E. Smith, X. Ke, Q. He, S. E. Daniels, *J. Phys. Chem.* **1993**, *97*, 10509 – 10512.
[80] M. Boiocchi, M. Bonizzoni, L. Fabbrizzi, F. Foti, M. Licchelli, A. Poggi, A. Taglietti, M. Zema, *Chem. Eur. J.* **2004**, *10*, 3209 – 3216.
[81] P. Thordarson, *Chem. Soc. Rev.* **2011**, *40*, 1305 – 1323.
[82] B. J. Deppmeier, A. J. Driessen, T. S. Hehre, W. J. Hehre, J. A. Johnson, P. E. Klunzinger, J. M. Leonard, I. N. Pham, W. J. Pietro, Y. Jianguo, Spartan '08, build 132 (Mar 27 2009),Wavefunction Inc., **2009**.
[83] Gaussian 09, Revision B.01, M. J. Frisch, G. W. Trucks, H. B. Schlegel, G. E. Scuseria, M. A. Robb, J. R. Cheeseman, G. Scalmani, V. Barone, B. Mennucci, G. A. Petersson, H. Nakatsuji, M. Caricato, X. Li, H. P. Hratchian, A. F. Izmaylov, J. Bloino, G. Zheng, J. L. Sonnenberg, M. Hada, M. Ehara, K. Toyota, R. Fukuda, J. Hasegawa, M. Ishida, T. Nakajima, Y. Honda, O. Kitao, H. Nakai, T. Vreven, J. A. Montgomery, Jr., J. E. Peralta, F. Ogliaro, M. Bearpark, J. J. Heyd, E. Brothers, K. N. Kudin, V. N. Staroverov, R. Kobayashi, J. Normand, K. Raghavachari, A. Rendell, J. C. Burant, S. S. Iyen-

gar, J. Tomasi, M. Cossi, N. Rega, J. M. Millam, M. Klene, J. E. Knox, J. B. Cross, V. Bakken, C. Adamo, J. Jaramillo, R. Gomperts, R. E. Stratmann, O. Yazyev, A. J. Austin, R. Cammi, C. Pomelli, J. W. Ochterski, R. L. Martin, K. Morokuma, V. G. Zakrzewski, G. A. Voth, P. Salvador, J. J. Dannenberg, S. Dapprich, A. D. Daniels, Ö. Farkas, J. B. Foresman, J. V. Ortiz, J. Cioslowski, D. J. Fox, Gaussian, Inc., Wallingford CT, **2009**.

[84] Y. Li, K. M. Mullen, T. D. W. Claridge, P. J. Costa, V. Felix, P. D. Beer, *Chem. Commun.* **2009**, *0*, 7134 – 7136.

[85] G. S. Manning, *Eur. Phys. J. E: Soft Matter Biol. Phys.* **2011**, *34*, 1 – 18.

[86] J. Ray, G. S. Manning, *Langmuir* **1994**, *10*, 2450 – 2461.

[87] A. Varghese, R. Rajesh, S. Vemparala, *J. Chem. Phys.* **2012**, *137*, 234901 – 234906.

[88] E. O. Stejskal, J. E. Tanner, *J. Chem. Phys.* **1965**, *42,* 288 – 292.

[89] E. F. Pettersen, T. D. Goddard, C. C. Huang, G. S. Couch, D. M. Greenblatt, E. C. Meng, T. E. Ferrin, *J. Comput. Chem.* **2004**, *25*, 1605 – 1612.

Received: December 11, 2013
Published online on April 30, 2014